Supporting Information

Colloidal Solution Combustion Synthesis: Toward Mass Production of a Crystalline Uniform Mesoporous CeO_2 Catalyst with Tunable Porosity

Albert A. Voskanyan, Kwong-Yu Chan*, Chi-Ying Vanessa Li

Department of Chemistry, The University of Hong Kong, Pokfulam Road, Hong Kong.

*Email: hrsccky@hku.hk

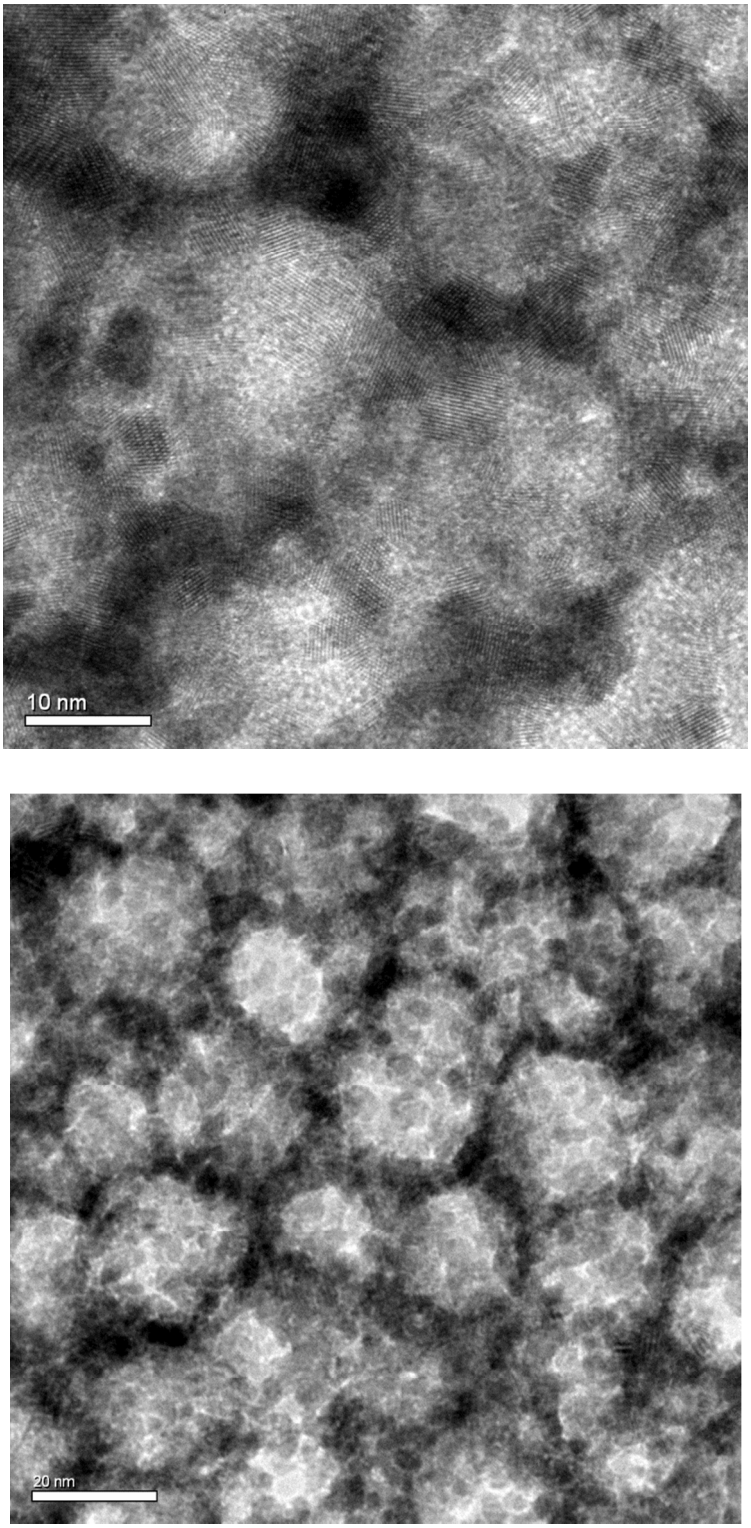

Figure S1. TEM images of ceria-3 sample at different magnifications.

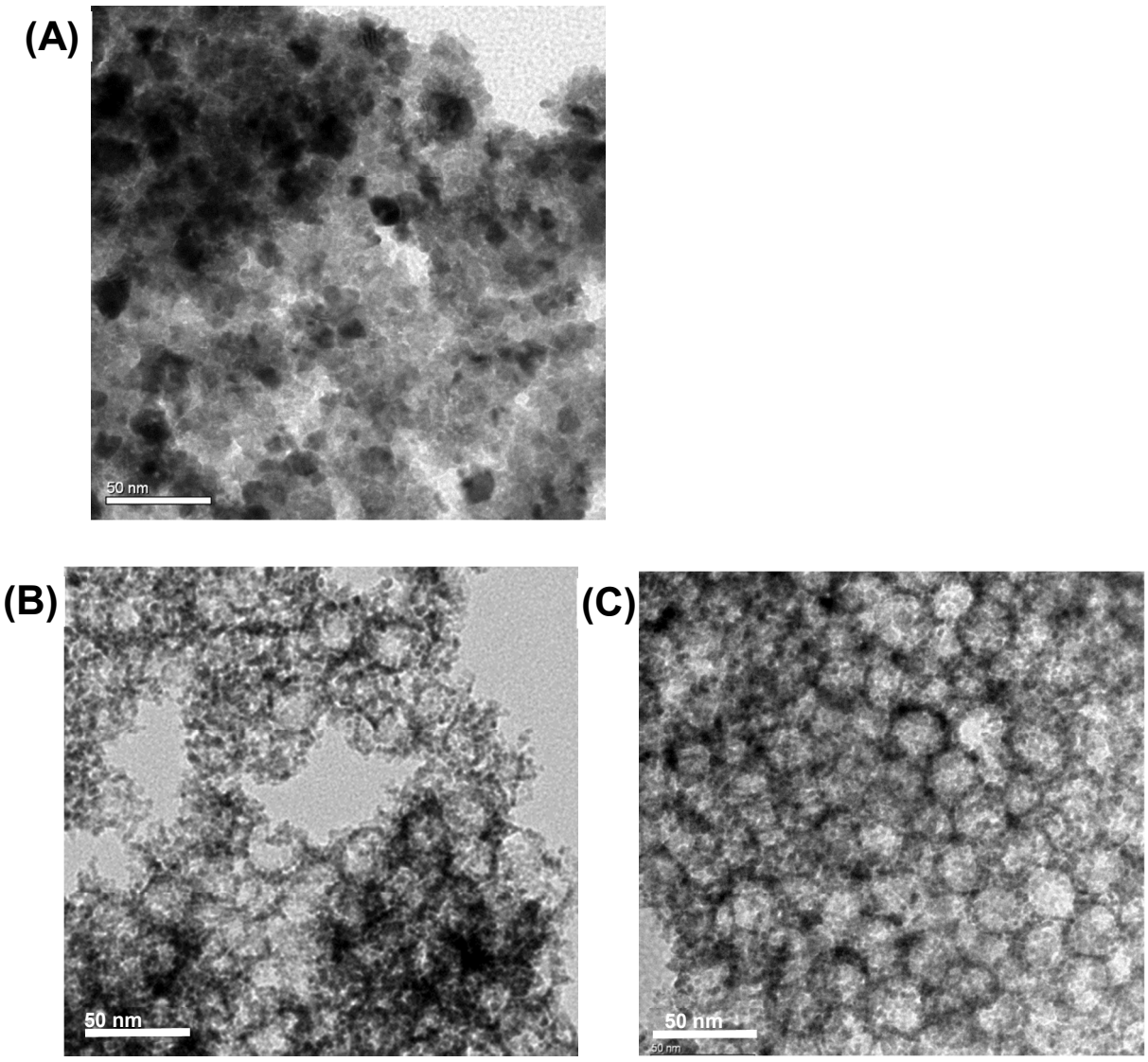

Figure S2. TEM images of (A) ceria-0, (B) ceria-1, (c) ceria-2 samples.

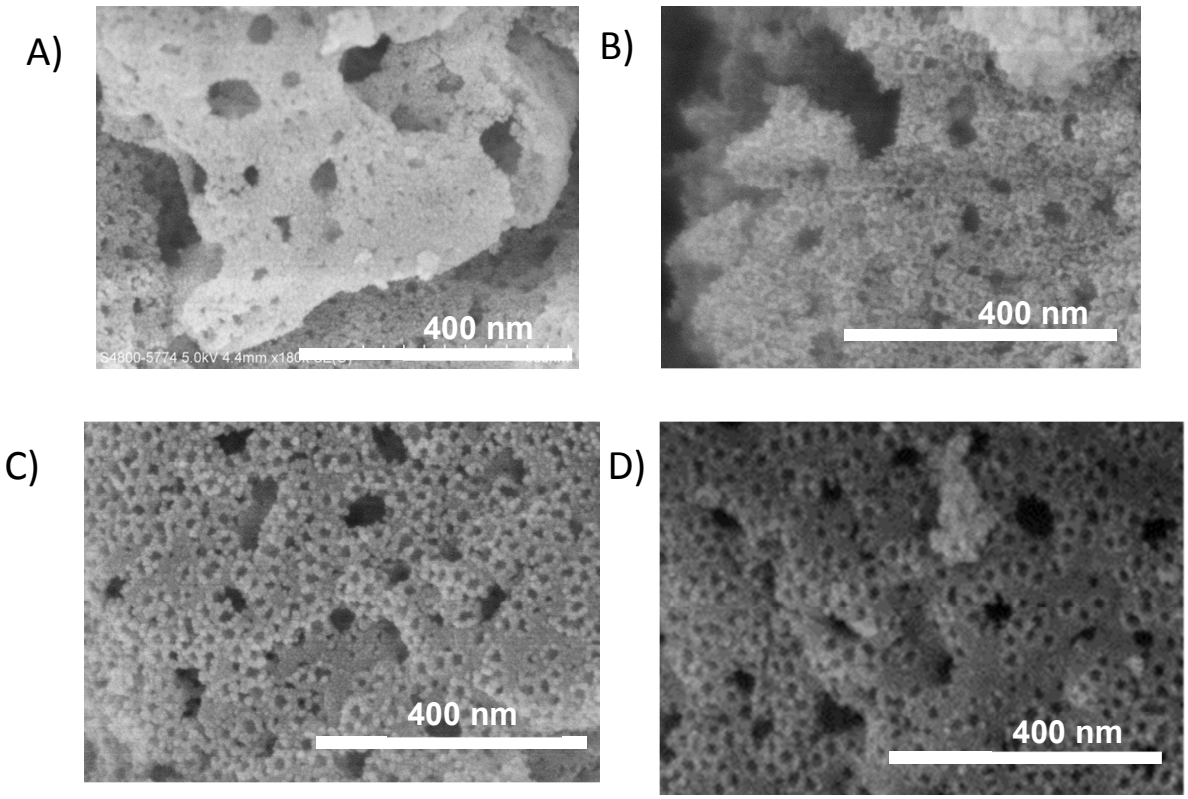

Figure S3. SEM images of different CeO_2 samples (A) ceria-0, (B) ceria-1, (C) ceria-2, and (D) ceria-3.

Porosity calculation

$m(CeO_2) = \rho_{CeO2} (V_{CeO2} - V_p)$ $V_p = 0.6$ ml $\rho(CeO_2)$ [ref.1] = 7.28 g ml^{-1}

After solving equation for 1 g of CeO_2 $V_{CeO2} = 0.74$ ml

Porosity = $\frac{Vp}{V_{CeO2}} \times 100\% = 81\%$

In CeO_2 Ce^{4+} is surrounded by eight O^{2-} ions. Formation of the oxygen vacancies and the accompanying Ce^{3+} reduces the coordination number of cerium from eight to seven causing the change in the Ce-O bond length and overall lattice constant. Also Ce^{3+} has a higher ionic radius (1.034 Å) compared to the Ce^{4+} (0.92 Å).

Figure S4 compares the Ce 3d core-level of three samples. Distinct photopeaks of CeO_2 are identified in the XPS spectra and labeled in accordance with the literature. The V and U labels refer to the $3d_{5/2}$ (Ce^{3+}) and $3d_{3/2}$ (Ce^{4+}) spin-orbit split components, respectively. The main peaks of V''' and U''' represented the $3d^{10}$ $4f^0$ initial electronic state corresponding to the Ce^{4+} cation whereas the peak of V' represented the $3d^{10}$ $4f^1$ initial electronic state of corresponding to the Ce^{3+} cation. The relative concentration of Ce^{3+} was calculated as[ref.2,3]:

$$(Ce^{3+}) = \frac{A_{v0} + A_{v\prime} + A_{u0} + A_{u\prime}}{A_{v0} + A_{v\prime} + A_{u0} + A_{u\prime} + A_v + A_u + A_{v\prime} + A_{u\prime} + A_{v\prime\prime} + A_{u\prime\prime} + A_{v\prime\prime\prime} + A_{u\prime\prime\prime}}$$

where A_i is the integrated area of peak í.

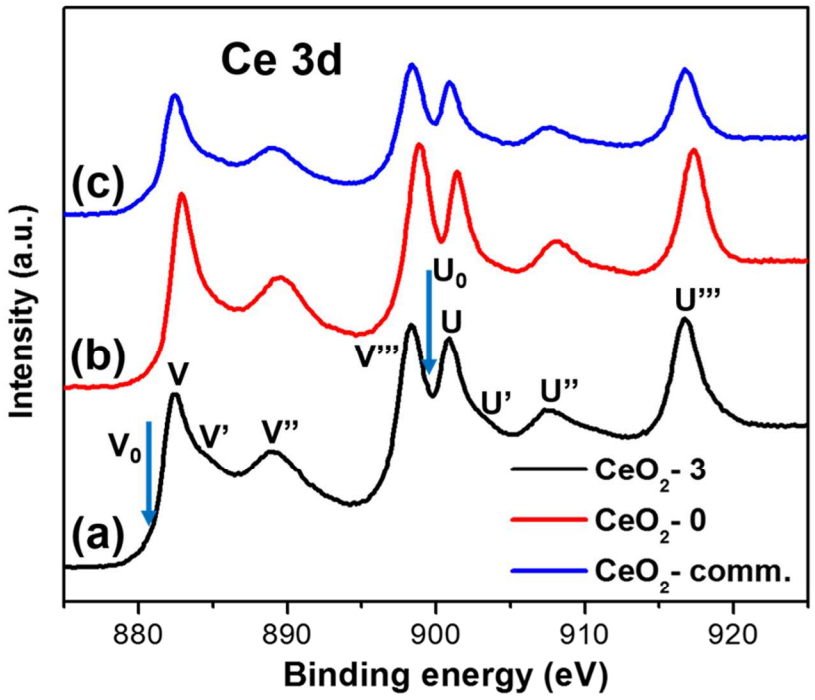

Figure S4. XPS of Ce 3d core level of different CeO_2 samples.

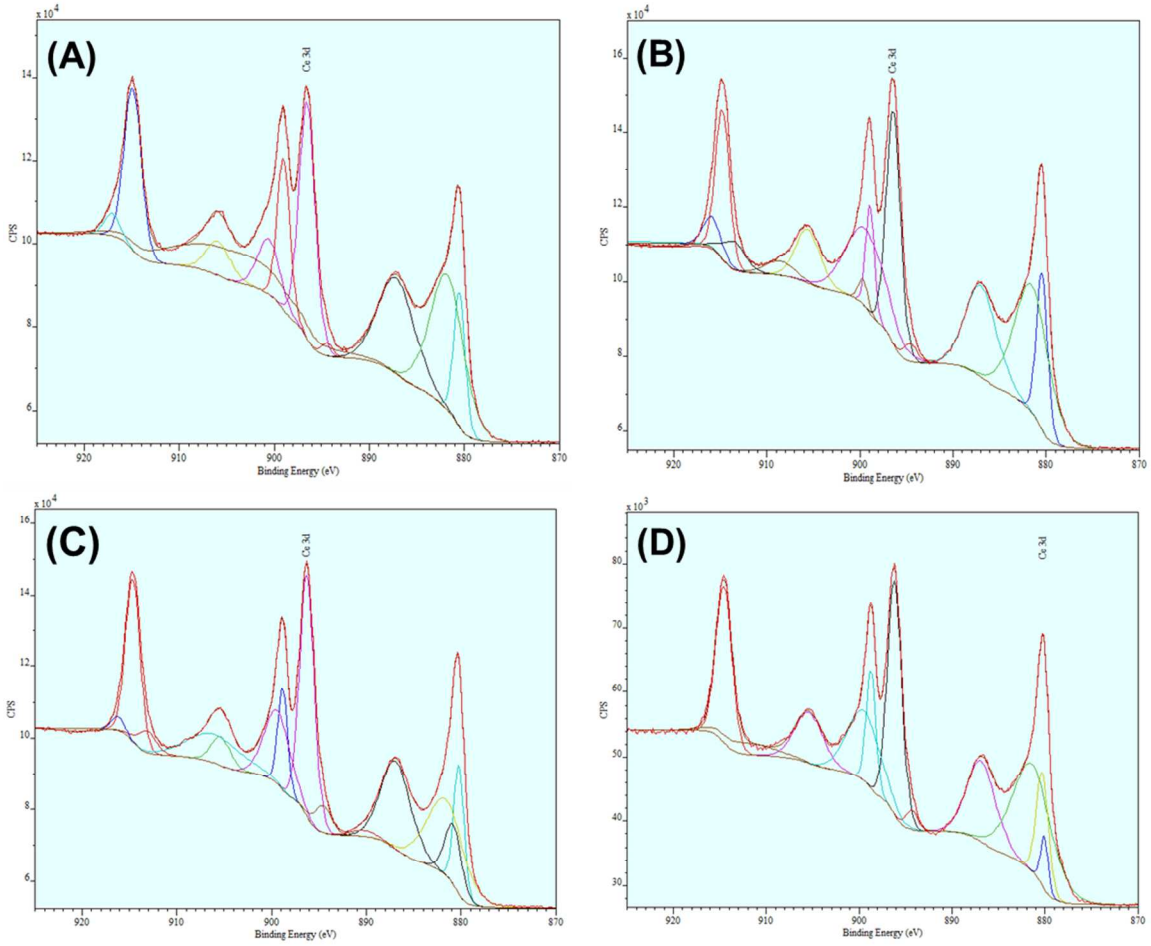

Figure S5. De-convoluted Ce 3d core level peaks of different CeO_2 samples (A) ceria-3, (B) ceria-2, (C) ceria-0, (D) ceria-comm.

To better understand the surface structure the O 1s peak is also analyzed for all samples (Figure S10). The O 1s peaks could be fitted into two peaks referred to as the lattice oxygen O^{2-} and the chemisorbed OH^- groups. The results in Table S2 also show that the concentration of adsorbed OH^- is the highest on the CeO_2-3 surface compared to other ceria samples. Emphatically, there is an additional third peak in O 1s region ascribed to the adsorbed H_2O molecules. The presence of the third peak can be due to the small particle size and high specific surface area leading to surface hydration.

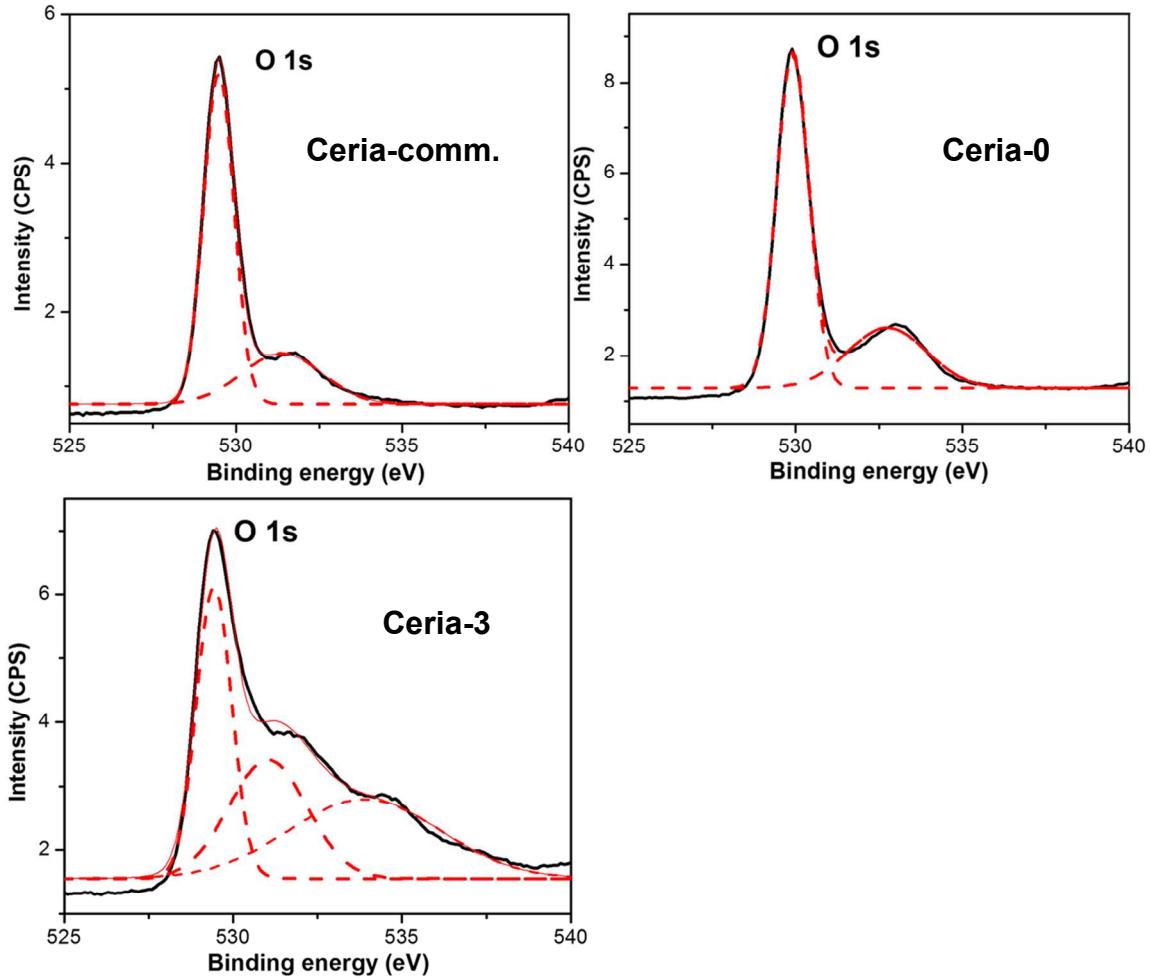

Figure S6. XPS of O 1s level of different CeO_2 samples.

Table S1. XPS results for the different CeO_2 samples

Sample	ceria-0	ceria-2	ceria-3	Commercial ceria
Volume of SiO_2 added (ml)	0	0.5	1	-
Concentration of Ce^{3+} ions (%)	6.1	25.8	34.9	1.3
OH^-/Total oxygen species (%)	20.53	38.26	39.75(+12.8)	16.96

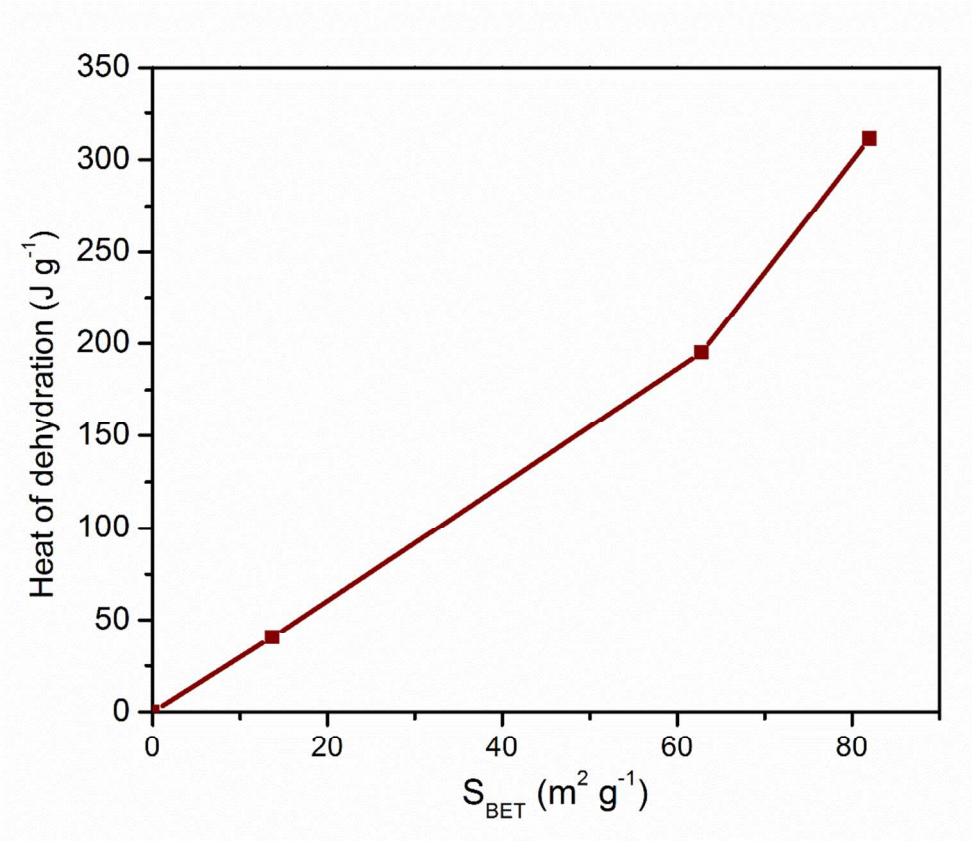

Figure S7. Heat of dehydration versus specific surface area of CeO_2.

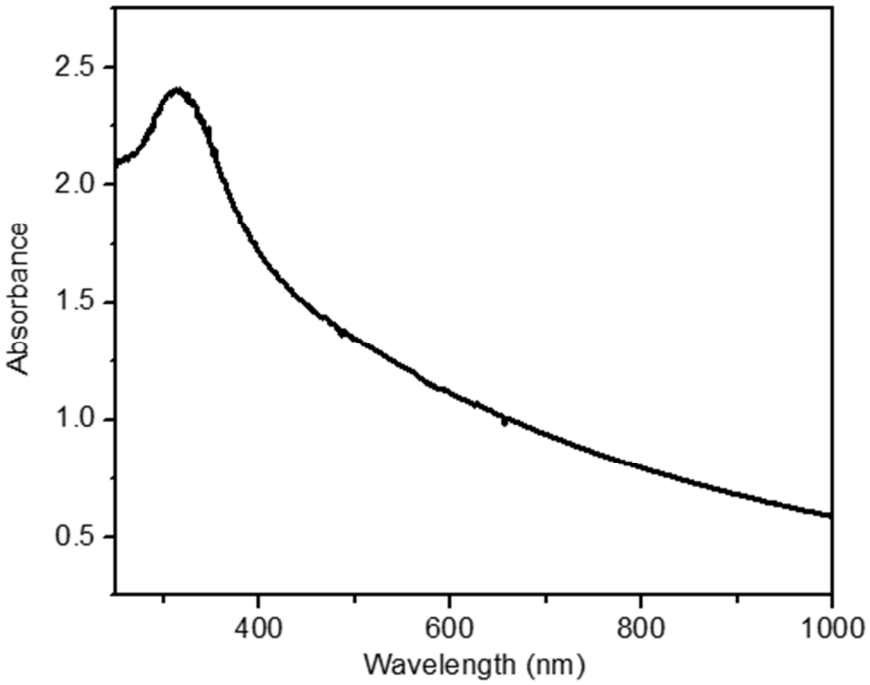

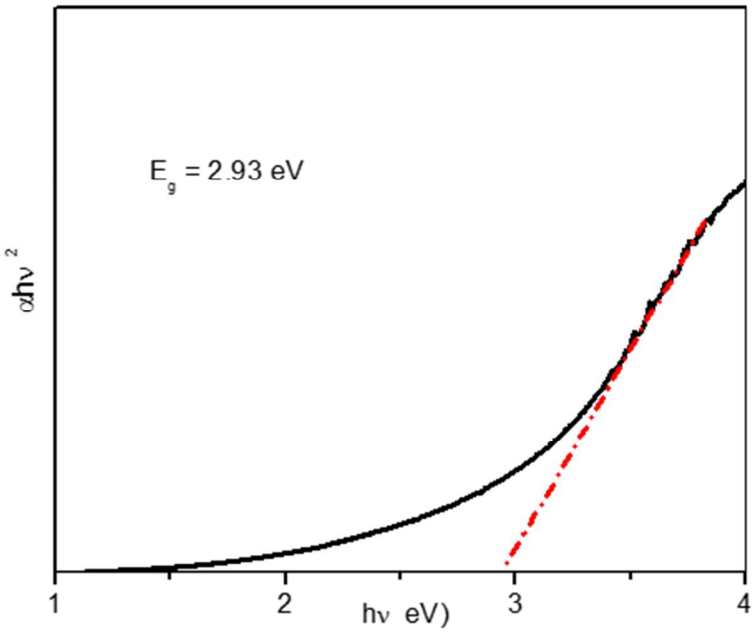

Figure S8. UV/vis absorption spectra and the plot of $(\alpha h\nu)^2$ versus photon energy for ceria-3.

References

(1) Wang Z.; Quan Z.; Lin J. Remarkable changes in the optical properties of CeO_2 nanocrystals induced by lanthanide ions doping. Inorg. Chem. **2007**, 46, 5237-5242.

(2) Desphande S.; Patil S.; Kuchibatla S. V. N. T.; Seal S. Size dependency variation in lattice parameter and valency states in nanocrystalline cerium oxide. Appl. Phys. Lett. **2005,** 87, 133113-3.

(3) Paparazzo E. On the curve-fitting of XPS Ce (3d) spectra of cerium oxides. Mater. Res. Bull. **2011**, 46, 323-326.